Nonlinear high-temperature superconducting terahertz metamaterials

2013 New J. Phys. 15 105016

(http://iopscience.iop.org/1367-2630/15/10/105016)

New Journal of Physics
The open access journal for physics

Nonlinear high-temperature superconducting terahertz metamaterials

Nathaniel K Grady[1], Bradford G Perkins Jr[2,3], Harold Y Hwang[2], Nathaniel C Brandt[2], Darius Torchinsky[2], Ranjan Singh[1], Li Yan[1], Daniel Trugman[1], Stuart A Trugman[1], Q X Jia[1], Antoinette J Taylor[1], Keith A Nelson[2] and Hou-Tong Chen[1,4]

[1] Center for Integrated Nanotechnologies, Los Alamos National Laboratory, Los Alamos, NM 87545, USA
[2] Department of Chemistry, Massachusetts Institute of Technology, Cambridge, MA 02139, USA
E-mail: chenht@lanl.gov

New Journal of Physics **15** (2013) 105016 (12pp)
Received 25 March 2013
Published 18 October 2013
Online at http://www.njp.org/
doi:10.1088/1367-2630/15/10/105016

Abstract. We report the observation of a nonlinear terahertz response of split-ring resonator arrays made of high-temperature superconducting films. Intensity-dependent transmission measurements indicate that the resonance strength decreases dramatically (i.e. transient bleaching) and the resonance frequency shifts as the intensity is increased. Pump–probe measurements confirm this behaviour and reveal dynamics on the few-picosecond timescale.

[3] Present address: MIT Lincoln Laboratory, 244 Wood Street, Lexington, MA 02420-9108, USA.
[4] Author to whom any correspondence should be addressed.

Contents

1. Introduction

Metamaterials consisting of arrays of conducting elements are a powerful tool for controlling electromagnetic energy in frequency ranges such as the terahertz (THz) spectrum where natural materials have limited functionalities [1, 2], and to create materials exhibiting exotic electromagnetic phenomena not observed in natural materials (e.g. negative refraction) [3–9]. Typically, metals are used as the conductive elements in metamaterial structures. However, because the intrinsic conductivity of a metal is difficult to influence, schemes for actively controlling the electromagnetic response of metamaterials generally focus on changing the environment around the metal. For example, one approach is to embed semiconducting elements in the metamaterial structure, exploiting the fact that an applied voltage or optical field can control the conductivity and dielectric constant of the semiconductor [10, 11]. This can dramatically alter the resonance strength and/or frequency of the metallic structures yielding an 'active' metamaterial.

While metals have been used for the conductive elements in the vast majority of metamaterial structures, the use of superconductors is of rapidly growing interest. In contrast to metals, the complex conductivity of superconductors intrinsically depends on the magnetic field, temperature, and applied optical fields [12–17]. Active metamaterial structures [14, 15, 17, 18] can therefore be realized by directly controlling the conductivity of the superconducting elements without introducing additional elements. In addition, superconductors exhibit superior conductivity at low temperatures and the potential to integrate elements exhibiting quantum behaviour.

While the nonlinear response of superconductors to high static magnetic fields, quasi-dc currents, and RF fields has been intensely studied [12, 18–28], only a few experiments have been reported in the THz frequency range [24, 29–31]. Measurements with ultrafast THz pulses have two important advantages over lower frequency measurements: the short pulses enable high field strengths to be reached without a high average power dissipation and the short timescale does not allow for the formation of vortices, which eliminates the two effects that have made observation of the intrinsic depairing current difficult at lower frequencies [19–22, 26, 28, 32]. Orenstein *et al* [24] measured the nonlinear transmission of BSSCO at modest field strengths using THz pulses generated by photoexcitation of voltage-biased GaAs, finding a characteristic current scale for the nonlinearity on the order of the intrinsic depairing current for BSSCO

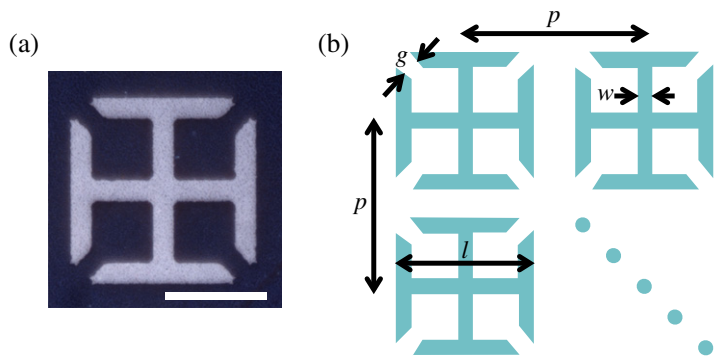

Figure 1. (a) Micrograph of one representative SRR where the light area is YBCO and the dark background is the LAO substrate. The scale bar is 20 μm. (b) Schematic diagram of the metamaterial. The dimensions are $g = 4\,\mu$m, $w = 4\,\mu$m, $l = 36\,\mu$m, and $p = 46\,\mu$m.

calculated from well-known parameters. Based on the observed scale of the limiting current, and the temperature and current dependence of the transmission they concluded that they were indeed measuring the intrinsic effects arising from the large superfluid velocities. However, the THz field intensity achievable with this method limited the maximum induced currents to an order of magnitude below the depairing current.

Recently developed high intensity THz sources based on tilted-pulse-front optical rectification are opening up new windows into the nonlinear response of materials in the THz frequency range [31, 33, 34]. These new high intensity sources, which can easily drive THz frequency/ps timescale currents exceeding the intrinsic depairing current in superconducting films, have enabled a resurgence of interest in the THz field induced nonlinear electrodynamics of superconductors. Using this approach, Zhang *et al* measured a field-induced nonlinear response of metamaterials and unpatterned films made out of the low-T_c conventional s-wave superconductor NbN [30, 31]. Similarly, Glossner *et al* measured the nonlinear transmission through films composed of the high-T_c d-wave superconductor $YBa_2C_3O_{7-\delta}$ (YBCO) [29]. Studying both types of superconductors is critical for developing a fundamental understanding of the THz field induced nonlinear effects because the presence of nodes in the superconducting gap can dramatically alter the behaviour [25, 27, 35–38] while observation of similar effects in both types of superconductors points towards a physical mechanism that does not require the presence of nodes. Further, the relaxation times are expected to be significantly different in these materials [26], which may have a significant effect for measurements on the ps timescale [39]. Here we exploit these recent advances in generating high intensity THz fields to study the intrinsic nonlinear response of metamaterials made out of YBCO. In contrast to previous measurements [24, 29], we exploit the enhanced sensitivity provided by resonant metamaterials to investigate the nonlinear response of YBCO and measure the dynamics associated with this response.

2. Metamaterial design and fabrication

Our sample consists of an array of electric split-ring resonators (SRR), shown in figure 1, made from a 100 nm thick epitaxial YBCO superconductor film deposited by pulsed-laser deposition

onto a 0.5 mm thick $LaAlO_3$ (LAO) substrate. To deposit YBCO films, we used an ArF excimer laser operating at an energy density on the target surface of $2\,J\,cm^{-2}$. The substrate temperature during the deposition was initially optimized and maintained at 775 °C. The YBCO film on LAO deposited under optimal conditions was of high quality epitaxy with a transition temperature of $T_c \approx 90\,K$. The YBCO film is oriented with the crystallographic *ab* plane parallel to the surface. The SRRs used here, identical to those used in our previous studies of temperature and optical tuning of superconducting metamaterials [13, 17], are designed to have a polarization-independent electric response due to the symmetry of the unit cell [40, 41]. The choice of SRR design is not essential to the results presented here and we expect similar results for other resonant structures where the resonator is formed from the superconductor (although the case of complimentary structures [40], where the SRR is a hole in a continuous superconducting film, is less clear).

3. High intensity terahertz source

The metamaterial transmission was studied using a high-intensity THz time-domain spectroscopy apparatus configured for either high intensity transmission measurements or THz-pump/THz-probe measurements of the transmission dynamics as described in [33]. Briefly, THz radiation was produced by nonlinear rectification of ultrafast near-infrared (NIR) laser pulses from an amplified Ti:sapphire laser (centre wavelength = 800 nm, pulsewidth = 100 fs, energy = $6\,mJ\,pulse^{-1}$, repetition rate = 1 kHz) in 0.6% MgO doped stoichiometric $LiNbO_3$ (MgO:sLN). The NIR pulse front was tilted relative to the propagation direction to achieve a velocity matching between the optical and THz pulses in the $LiNbO_3$ and therefore a high optical rectification conversion efficiency. THz pulse energies achieved in this system are $\sim 2\,\mu J$ which, when focused tightly, yielded field strengths of $\sim 200\,kV\,cm^{-1}$ at the focus. The metamaterial sample and a reference LAO substrate were simultaneously mounted on the cold finger of a continuous flow liquid helium cryostat. Due to geometric constraints on the positioning of the cryostat within the apparatus, the sample was not quite at the focus reducing the peak THz field strength at the sample to approximately $45\,kV\,cm^{-1}$. For the pump–probe experiments, the optical pulse was split in two, and recombined nearly collinearly in the $LiNbO_3$ with a variable delay between the pulses. Electro-optical (EO) sampling in a ZnTe crystal was used to detect the pulses with a Si wafer attenuator used between the sample and the EO sampling crystal to prevent over-rotation at high THz field strengths. Spectra were obtained by applying a fast Fourier transform to the time-domain THz waveforms with a Hanning window to suppress spurious oscillations in the spectra due to the finite time window.

4. Intensity-dependent transmission measurements

First, we examine the intensity dependent transmission, shown in figure 2, at several temperatures ranging from 23 K, which is well below the superconducting transition temperature, to 90 K where the YBCO becomes a normal conductor. Two resonances are visible in the transmission spectra: the fundamental LC resonance due to the loop inductance and gap capacitance at ~0.5 THz and the collective dipolar resonance at ~1.2 THz [1, 7, 13, 40, 41]. It is immediately apparent that the resonances become weaker with both increasing temperature and, for a given temperature, increasing THz field strength.

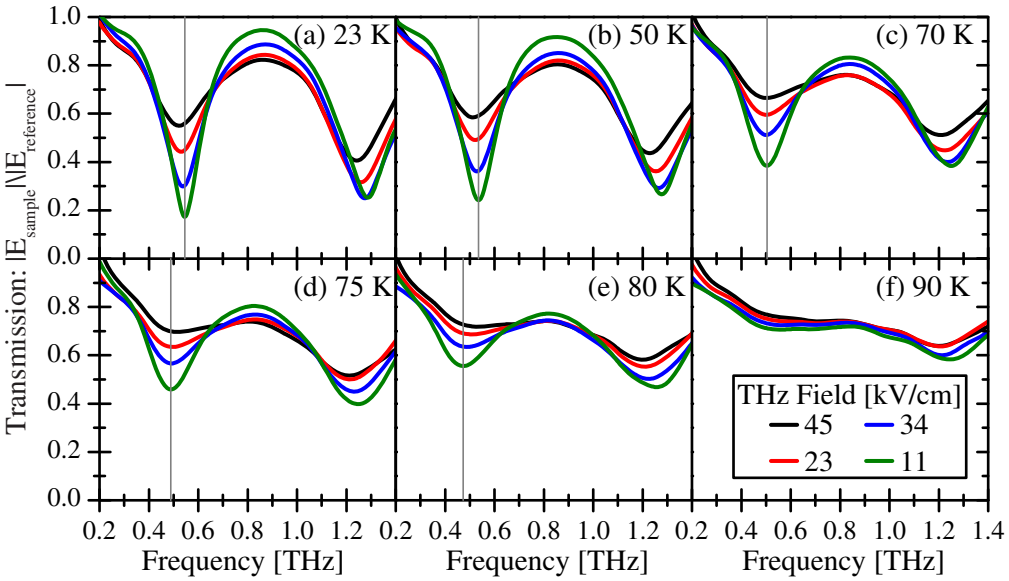

Figure 2. THz field strength dependent transmission through the metamaterial relative to an LAO reference substrate at several temperatures from 23 to 90 K. The thin vertical lines indicate the resonance frequency at 11 kV cm^{-1}.

A more quantitative picture can be obtained by extracting the transmission minimum and resonance frequency of the fundamental LC resonance around 0.5 THz, shown in figure 3. Note that for the 90 K spectra shown in figure 2(f), the resonance is not sufficiently well defined to reliably extract the resonance frequency so the 90 K data in figures 3(b) and (d) are evaluated at 0.51 THz for all field intensity. At low temperatures the fundamental LC resonance red-shifts with increasing pulse energy, while closer to T_c the resonance blue-shifts, similar to the behaviour discussed in our previous work on temperature tuning of a similar sample [17]. For all temperatures the transmission at the resonance increases with increasing incident intensity, indicating that the resonance is becoming weaker. The magnitude of this change is quite remarkable: at 23 K we observe a >10 dB change in transmission at the resonance and >5 dB as we approach liquid nitrogen temperatures. Due to the simultaneous frequency shift of the resonance, the change in transmission at a single frequency will be slightly higher than that shown in figure 3(b).

In figure 3(c) the per cent change of the resonance frequency caused by the intense THz field, defined as $(f_{LC}(11\,\mathrm{kV\,cm^{-1}})-f_{LC}(45\,\mathrm{kV\,cm^{-1}}))/f_{LC}(11\,\mathrm{kV\,cm^{-1}}) \times 100\%$, where $f_{LC}(E)$ is the LC resonance frequency at an incident field strength E is shown. Likewise, in figure 3(d) the per cent change in transmission at the LC resonance is shown. From a practical point of view, figure 3(d) indicates that for a device application operating at the lowest temperature is desirable. In contrast to the recent report by Glossner *et al* [29], who were unable to resolve any nonlinearity at or above T_c in the measured the transmission of high intensity THz pulses through unpatterened YBCO films, and Orenstein *et al* [24] who likewise observed 'nearly linear electrodynamics', near and above T_c, we observe a nonlinear response extending through the transition temperature. This highlights the high sensitivity provided by the resonant structures investigated here.

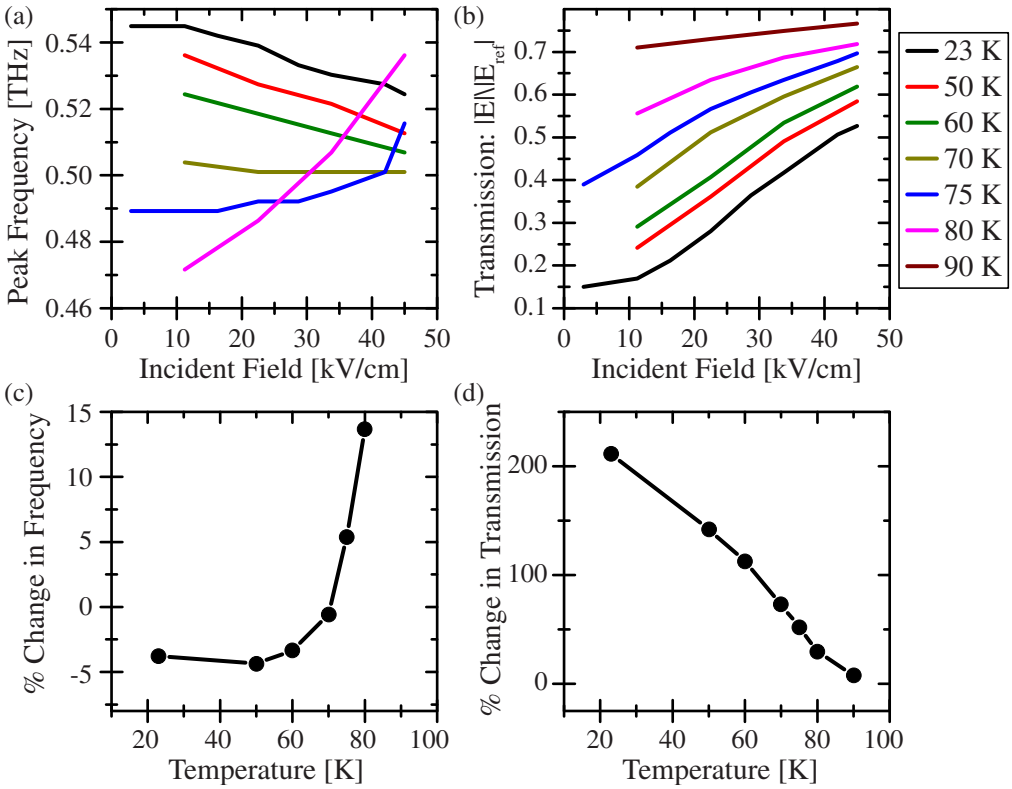

Figure 3. Incident field dependence of the (a) LC resonant frequency and (b) transmission minimum at the fundamental LC resonance. Per cent change of the (c) frequency of the LC resonance shown in (a), and (d) transmission at the LC resonance shown in (b) when the incident field is increased from 11 to 45 kV cm^{-1}.

5. Dynamics

To investigate the dynamics, we performed THz-pump/THz-probe measurements. For these measurements, the pump intensity was close to the maximum intensity used in the intensity-dependent transmission measurements presented in figures 2 and 3. The full transmission spectrum as a function of time is needed to unambiguously resolve the dynamics of the metamaterial resonance since it both shifts in frequency and changes amplitude. To obtain this, we vary the time delay τ between the pump and probe pulses and for each τ measure the transmitted electric field as a function of time. Applying a Fourier transform then yields the transmission spectrum at each pump–probe delay, which is shown in figure 4. The data from $\tau \sim -1.5$ to 1.5 ps should be ignored due to the influence of the overlapping optical pulses in the $LiNbO_3$ crystal on the generation of the pump and probe pulses. The finite substrate thickness limits the maximum pump–probe delay to ~11 ps, at which point the reflection of the pump pulse from the exit face of the substrate returns to the surface with the superconducting SRRs, introducing an additional perturbation.

The transmission spectrum as a function of time delay between the pump and probe pulses is shown as a density plot in figure 4(a) where each horizontal slice represents a transmission spectrum at a given time delay. To facilitate comparison with the

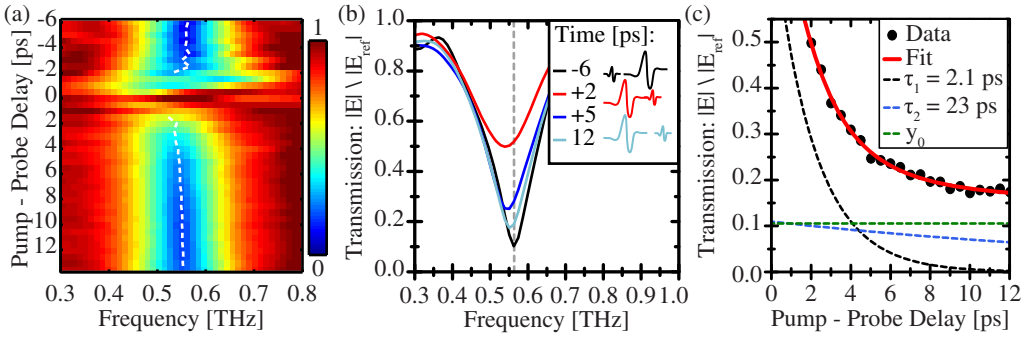

Figure 4. (a) Pump–probe transmission spectra for the sample at 23 K shown as a density plot where each horizontal slice is a spectrum at a given pump–probe delay. The white dashed line indicates the resonance frequency. (b) Transmission spectra at several representative pump–probe delays. (c) Transmission at the metamaterial resonance as a function of pump–probe delay with a bi-exponential fit. The two components of the exponential decay and offset are indicated separately with dashed lines. Positive delay corresponds to the probe pulse arriving at the sample after the pump pulse as illustrated in the legend of (b).

intensity-dependent transmission, the transmission spectra at selected time delays are shown figure 4(b). We find that the LC resonance shifts to higher energy and the transmission at the resonance decreases with increasing pump–probe delay. This is similar to the power-dependent spectra shown in figure 2(a), where the resonance shifts to higher frequency and becomes stronger with decreasing intensity.

Examining the transmission as a function of pump–probe delay, shown in figure 4(c), reveals that there is a strong increase in the transmission when the pump and probe pulses overlap followed by a rapid decrease with increasing pump–probe delay as the resonance recovers. The decay follows a bi-exponential behaviour, shown by the fit in figure 4(c), with time constants $\tau_1 = 2.1$ and $\tau_2 = 23$ ps. A linear offset is necessary in the fit because the low field transmission at the resonance is not zero.

6. Discussion

Previous work investigating the tuning of YBCO metamaterials by changing the temperature [17] or applying NIR light pulses [13], and the tuning of NbN metamaterials by applying intense THz fields [31] have shown that the changes in the metamaterial resonance are reasonably well described by the change in the complex conductivity of the constituent superconductor film. However, this still leaves open the question of what is the fundamental mechanism responsible for changing the conductivity of the superconductor in response to an intense THz field.

Both temperature and optical tuning arise from the change in the density of superconducting and normal carriers. It is well known that increasing the temperature of a superconductor decreases the density of superconducting Cooper pairs relative to the normal conduction electron population (until the Cooper pair density goes to 0 at T_c), which directly influences the conductivity of the superconductor [12]. Optical tuning of the superconductor

conductivity is also not surprising as the energy of a NIR photon is orders of magnitude greater than the condensation energy of the Cooper pairs and absorption of a photon can therefore easily break the Cooper pair into two hot quasiparticles. In contrast, the energy of a THz photon in the frequency range used in the present experiment is well below that required to directly break a Cooper pair upon absorption, nor do the applied THz pulses significantly raise the sample temperature.

We can gain some insight into the mechanism behind the observed nonlinearities by considering the two-fluid model where the conductivity of a superconductor is considered to be the combination of a Drude response due to the population of normal carriers and an accelerative supercurrent term due to the population of superconducting electrons (Cooper pairs) [12, 19, 22]. In the Drude model, electrons are accelerated by an applied uniform electric field for a characteristic time τ, after which the momentum is randomized by a scattering event. The motion of normal electrons can therefore be described by the classical equation of motion $\mathrm{d}(m\mathbf{v}_\mathrm{n})/\mathrm{d}t = e\mathbf{E}–m\mathbf{v}_\mathrm{n}/\tau$, where τ is a phenomenological relaxation time, m is the electron mass, e is the electron charge and $\mathbf{v}_\mathrm{n}$ is the electron velocity. The resulting normal current density is then $\mathbf{J_n} = n_\mathrm{n} e\mathbf{v}_\mathrm{n}$, where n_n is the density of normal electrons. In the London limit, the supercurrent is directly proportional to the centre of mass velocity of the superconducting electron condensate. In a uniform electric field the superconducting electrons will likewise be accelerated; however, the hallmark of superconductivity is that these electrons travel unimpeded through the superconducting medium as Cooper pairs. That is, the superconducting electrons gain momentum as $\mathrm{d}(m\mathbf{v}_\mathrm{s})/\mathrm{d}t = e\mathbf{E}$, where $\mathbf{v}_\mathrm{s}$ is the centre of mass velocity of the superconducting electron condensate. The resulting supercurrent is then $\mathbf{J_s} = n_\mathrm{s} e\mathbf{v}_\mathrm{s}$, where n_s is the density of superconducting electrons. This is essentially the first London equation [12]. We can straightforwardly evaluative these equations in the context of the present experiment by assuming the temporal variation and peak intensity of the electric field $E(t)$ matches the measured THz waveform, but neglecting the spatial variation of the field and assuming an infinite superconducting medium. The results of this calculation are shown in figure 5 where the properties of YBCO at 60 K are taken to be $n_\mathrm{n} = 4.6 \times 10^{26}\,\mathrm{m}^{-3}$, $n_\mathrm{s} = 6.7 \times 10^{26}\,\mathrm{m}^{-3}$ and $\tau = 0.41$ THz [16]. Note that evaluating the model at a lower temperature increases the peak supercurrent. While a very crude approximation, this model nonetheless provides some insight into the possible mechanisms behind the observed nonlinear response.

Similar to how the upper thermodynamic critical field H_{c2} is derived from considering when the energy required to expel the flux exceeds the condensation energy, there is a critical intrinsic depairing current j_d above which the kinetic energy density exceeds the condensation energy [12, 19–28, 32, 35–3942]. An excellent review of this derivation is given in [19]. This has been extensively studied in static fields as the nonlinear Meissner effect (NLME) and at microwave frequencies where it results in intermodulation effects. Much of the theoretical work considering the ac nonlinearity assume a small perturbing ac field probing a nonlinearity due to a high dc bias [12, 19, 21–26, 28, 32, 37, 39], which may not describe the present experiment where only a strong ac field is applied [24, 39]. There are two directions from which a more detailed picture of the mechanism responsible the depairing current (or NLME) is generally arrived at. Macroscopically, in the absence of spatial variations of the order parameter, there are two contributions to the free energy in the Ginzburg–Landau equations that act to counter the condensation energy: the magnetization and the kinetic energy of the supercurrents. This last term directly results in a kinetic energy dependence of the order parameter and therefore a velocity or current

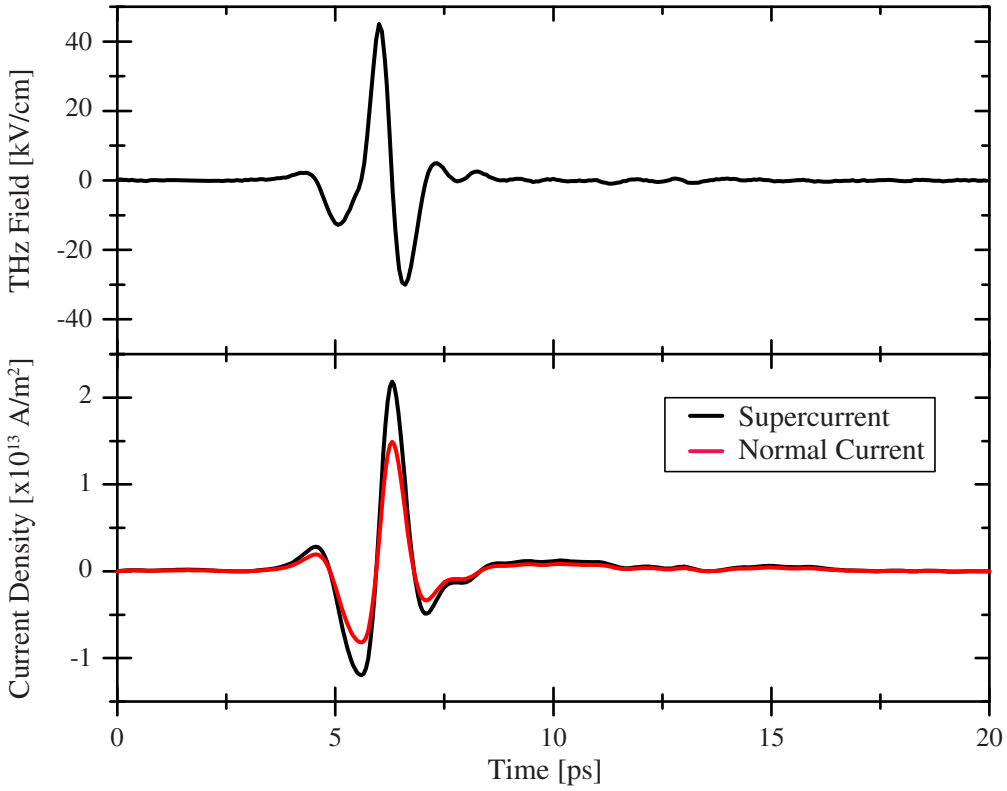

Figure 5. Current density induced by a high intensity THz field in the London limit.

dependent Cooper pair density [12, 23]. Microscopically, the thermally excited quasiparticle backflow current (or paramagnetic current) is Doppler-shifted relative to the supercurrent, reducing the effective superconducting gap as the supercurrent velocity increases. This reduction in the effective gap results in a decrease in the superfluid density with increasing velocity (i.e. the Cooper pair density decreases with increasing current) for both s- and d-wave superconductors. In an s-wave superconductor with an isotropic gap, this effect vanishes at $T = 0\,\mathrm{K}$ due to the lack of thermally excited quasiparticles. In a d-wave superconductor, the vanishing superconducting gap at the nodes both dramatically increases the magnitude of this effect, allows it to persist down to $T = 0\,\mathrm{K}$, and introduces a dependence on the in-plane field orientation [12, 19, 23–25]. However, it is important to keep in mind that because these theories may be inadequate to describe THz nonlinearities because they are derived in the quasistatic limit and therefore neglect mechanisms that only occur at high frequencies [24, 39]. For example, for fast pulses comparable to the order parameter relaxation time, order parameter relaxation has been predicted to give rise to an additional dissipative term, kinetic resistance, separate from that due to the normal carriers [39].

Measurements of the propagation of short current pulses through superconducting microbridges have shown that the critical depairing current for YBCO is $\sim 10^{12}\,\mathrm{A\,m^{-2}}$ [20, 21], which is far lower than the peak currents on the order of $10^{13}\,\mathrm{A\,m^{-2}}$ that the straightforward application of the two fluid model shown in figure 5 predicts for an applied field of $45\,\mathrm{kV\,cm^{-1}}$. While this simple model cannot provide a detailed comparison with the experimental measurements, it nonetheless provides insight into the mechanism behind the

observed nonlinearities by providing a clear indication that the THz fields considered here are well into the regime where significant nonlinearities due to kinetic energy induced pair breaking would be expected. We are presently working towards developing a more detailed model of the nonlinear response that can be applied to modelling superconducting THz metamaterials.

7. Conclusion

In conclusion, we have observed strong nonlinearities in the THz response of metamaterials fabricated from thin, high-T_c superconducting films. These observations are not only of practical interest for developing active and nonlinear metamaterial devices, but also of fundamental interest due to their potential to improve our understanding of the physics of high-T_c superconductivity.

Acknowledgments

We acknowledge partial support from the Los Alamos National Laboratory's Laboratory Directed Research and Development (LDRD) programme and the Office of Naval Research (ONR) grant N00014-09-1-1103. This work was performed, in part, at the Center for Integrated Nanotechnologies, a user facility of the Office of Basic Energy Sciences. Los Alamos National Laboratory, an affirmative action equal opportunity employer, is operated by Los Alamos National Security, LLC, for the National Nuclear Security Administration of the US Department of Energy under contract DE-AC52-06NA25396. BGP acknowledges the National Science Foundation for support though the American Competitiveness in Chemistry Fellowship (ACC-F) 1041979.

References

[1] Chen H T, O'Hara J F, Azad A K and Taylor A J 2011 Manipulation of terahertz radiation using metamaterials *Laser Photon. Rev.* **5** 513–33
[2] Ferguson B and Zhang X C 2002 Materials for terahertz science and technology *Nature Mater.* **1** 26–33
[3] Pendry J B, Schurig D and Smith D R 2006 Controlling electromagnetic fields *Science* **312** 1780–2
[4] Shalaev V M, Cai W S, Chettiar U K, Yuan H K, Sarychev A K, Drachev V P and Kildishev A V 2005 Negative index of refraction in optical metamaterials *Opt. Lett.* **30** 3356–8
[5] Shelby R A, Smith D R and Schultz S 2001 Experimental verification of a negative index of refraction *Science* **292** 77–9
[6] Smith D R, Padilla W J, Vier D C, Nemat-Nasser S C and Schultz S 2000 Composite medium with simultaneously negative permeability and permittivity *Phys. Rev. Lett.* **84** 4184–7
[7] Zheludev N I and Kivshar Y S 2012 From metamaterials to metadevices *Nature Mater.* **11** 917–24
[8] Yu N, Genevet P, Kats M A, Aieta F, Tetienne J-P, Capasso F and Gaburro Z 2011 Light propagation with phase discontinuities: generalized laws of reflection and refraction *Science* **334** 333–7
[9] Grady N K, Heyes J E, Chowdhury D R, Zeng Y, Reiten M T, Azad A K, Taylor A J, Dalvit D A R and Chen H-T 2013 Terahertz metamaterials for linear polarization conversion and anomalous refraction *Science* **340** 1304–7
[10] Chen H T, Padilla W J, Zide J M O, Gossard A C, Taylor A J and Averitt R D 2006 Active terahertz metamaterial devices *Nature* **444** 597–600
[11] Chen H-T, O'Hara J F, Azad A K, Taylor A J, Averitt R D, Shrekenhamer D B and Padilla W J 2008 Experimental demonstration of frequency-agile terahertz metamaterials *Nature Photon.* **2** 295–8

[12] Tinkham M 1996 *Introduction to Superconductivity* 2nd edn (Mineola, NY: Dover)
[13] Singh R, Xiong J, Azad A K, Yang H, Trugman S A, Jia Q X, Taylor A J and Chen H-T 2012 Optical tuning and ultrafast dynamics of high-temperature superconducting terahertz metamaterials *Nanophotonics* **1** 117–23
[14] Ricci M C, Xu H, Prozorov R, Zhuravel A P, Ustinov A V and Anlage S M 2007 Tunability of superconducting metamaterials *IEEE Trans. Appl. Supercond.* **17** 918–21
[15] Zhang C H, Wu J B, Jin B B, Ji Z M, Kang L, Xu W W, Chen J, Tonouchi M and Wu P H 2012 Low-loss terahertz metamaterial from superconducting niobium nitride films *Opt. Express* **20** 42–7
[16] Pimenov A, Loidl A, Jakob G and Adrian H 1999 Optical conductivity in $YBa_2Cu_3O_{7-\delta}$ thin films *Phys. Rev.* B **59** 4390–3
[17] Chen H-T, Yang H, Singh R, O'Hara J F, Azad A K, Trugman S A, Jia Q X and Taylor A J 2010 Tuning the resonance in high-temperature superconducting terahertz metamaterials *Phys. Rev. Lett.* **105** 247402
[18] Savinov V, Fedotov V A, Anlage S M, Groot P A J d and Zheludev N I 2012 Modulating sub-THz radiation with current in superconducting metamaterial *Phys. Rev. Lett.* **109** 243904
[19] Kunchur M N 2004 Current-induced pair breaking in magnesium diboride *J. Phys.: Condens. Matter* **16** R1183–204
[20] Kunchur M N, Christen D K, Klabunde C E and Phillips J M 1994 Pair-breaking effect of high current densities on the superconducting transition in $YBa_2Cu_3O_{7-\delta}$ *Phys. Rev. Lett.* **72** 752–5
[21] Lang W, Puica I, Peruzzi M, Lemmermann K, Pedarnig J D and Bäuerle D 2005 Depairing current and superconducting transition of YBCO at intense pulsed currents *Phys. Status Solidi* c **2** 1615–24
[22] Saracila G F and Kunchur M N 2009 Ballistic acceleration of a supercurrent in a superconductor *Phys. Rev. Lett.* **102** 077001
[23] Bardeen J 1962 Critical fields and currents in superconductors *Rev. Mod. Phys.* **34** 667–81
[24] Orenstein J, Bokor J, Budiarto E, Corson J, Mallozzi R, Bozovic I and Eckstein J N 1997 Nonlinear electrodynamics in cuprate superconductors *Physica* C **282–287** (Pt 1) 252–5
[25] Yip S K and Sauls J A 1992 Nonlinear Meissner effect in CuO superconductors *Phys. Rev. Lett.* **69** 2264–7
[26] Golosovsky M 1998 Physical mechanisms causing nonlinear microwave losses in High-T_c superconductors *Part. Accelerators* **61** 87–106
[27] Zhuravel A P, Ghamsari B G, Kurter C, Jung P, Remillard S, Abrahams J, Lukashenko A V, Ustinov A V and Anlage S M 2013 Imaging the anisotropic nonlinear meissner effect in nodal $YBa_2Cu_3O_{7-\delta}$ thin-film superconductors *Phys. Rev. Lett.* **110** 087002
[28] Samoilova T B 1995 Non-linear microwave effects in thin superconducting films *Supercond. Sci. Technol.* **8** 259–78
[29] Glossner A, Zhang C, Kikuta S, Kawayama I, Murakami H, Müller P and Tonouchi M 2012 Cooper pair breakup in $YBa_2Cu_3O_{7-\delta}$ under strong terahertz fields arXiv:1205.1684v1
[30] Zhang C *et al* 2013 Nonlinear response of superconducting NbN thin film and NbN metamaterial induced by intense terahertz pulses *New J. Phys.* **15** 055017
[31] Zhang C, Jin B, Han J, Kawayama I, Murakami H, Wu J, Kang L, Chen J, Wu P and Tonouchi M 2013 Terahertz nonlinear superconducting metamaterials *Appl. Phys. Lett.* **102** 081121
[32] Geier A and Schön G 1982 Response of a superconductor to a supercritical current pulse *J. Low Temp. Phys.* **46** 151–60
[33] Hoffmann M C, Hebling J, Hwang H Y and Nelson K-L Y K A 2009 THz-pump/THz-probe spectroscopy of semiconductors at high field strengths *J. Opt. Soc. Am.* B **26** A29–34
[34] Liu M *et al* 2012 Terahertz-field-induced insulator-to-metal transition in vanadium dioxide metamaterial *Nature* **487** 345–8
[35] Dahm T and Scalapino D J 1996 Theory of microwave intermodulation in a high-T_c superconducting microstrip resonator *Appl. Phys. Lett.* **69** 4248–50
[36] Dahm T and Scalapino D J 1997 Theory of intermodulation in a superconducting microstrip resonator *J. Appl. Phys.* **81** 2002–9

[37] Žutić I and Valls O T 1997 Superconducting-gap-node spectroscopy using nonlinear electrodynamics *Phys. Rev.* B **56** 11279–93
[38] Zare A, Dahm T and Schopohl N 2010 Strong surface contribution to the nonlinear Meissner effect in d-wave superconductors *Phys. Rev. Lett.* **104** 237001
[39] Clem J R and Kogan V G 2012 Kinetic impedance and depairing in thin and narrow superconducting films *Phys. Rev.* B **86** 174521
[40] Chen H-T, O'Hara J F, Taylor A J, Averitt R D, Highstrete C, Lee M and Padilla W J 2007 Complementary planar terahertz metamaterials *Opt. Express* **15** 1084–95
[41] Padilla W J, Aronsson M T, Highstrete C, Lee M, Taylor A J and Averitt R D 2007 Electrically resonant terahertz metamaterials: theoretical and experimental investigations *Phys. Rev.* B **75** 041102
[42] Nicol E J and Carbotte J P 2006 Effect of gap suppression by superfluid current on the nonlinear microwave response of d-wave superconductors *Phys. Rev.* B **73** 174510